Research Article

iMedPub Journals
http://www.imedpub.com

Nano Research & Applications
ISSN 2471-9838

2017
Vol. 3 No. 2 : 9

DOI: 10.21767/2471-9838.100026

The Study of Structural, Physical and Electrochemical Activity of Zno Nanoparticles Synthesized by Green Natural Extracts of *Sageretia Thea*

Noluthando Mayedwa[1]*, Ali Talha Khalil[3], Nametso Mongwaketsi[1], Nolubabalo Matinise[2], Zabta Khan Shinwari[3] and Malik Maaza[1,2]

1 iThemba Laboratories for Accelerator Based Science, Somerset West- 7129, South Africa

2 College of Graduate Studies, University of South Africa, UNESCO-Africa Chair in Nanoscience and Nanotechnology, Theo Van Wyk Building 9-119, South Africa.

3 Department of Biotechnology, Quaid-i-Azam University, 45320, Islamabad, Pakistan. Pakistan Academy of Science, 44000, UNSECO-Africa Chair in Nanoscience and Nanotechnology, NANOAFNET.

Corresponding author:
Noluthando Mayedwa

nmyedi@gmail.com

iThemba Laboratories for Accelerator Based Science, P. O Box 722, Somerset West, 7129, South Africa.

Tel: +27 (21) 843 1000

Citation: Mayedwa N, Khalil AT, Mongwaketsi N, et al. The Study of Structural, Physical and Electrochemical Activity of Zno Nanoparticles Synthesized by Green Natural Extracts of Sageretia Thea. Nano Res Appl. 2017, 3:2.

Abstract

In this contribution an exceptionally simple, cost effective and reliable method for biosynthesis of ZnO nanoparticles through using *Sageretia thea* natural extracts as an effective chelating agent. The morphological analysis shows ZnO has nanoscale particles size 28.09 nm ± 5 nm, crystalline and possess distinct nanostructure hexagonal wurtzite structure. Effects of heat on ZnO synthesised at room temperature caused bonds with in the molecule to be broken exhibited continuous weight loss with 3 quasi sharp changes and 3 endothermic peaks occurring at 79°C, 228°C and 300°C. A proposed mechanism of reaction for $Zn(NO_3)_2$ $6H_2O$ precursor with bioactive compounds in *Sageretia thea* extract such as phenolic acid, flavonoids, natural sterolin and vitamin based compounds to form ZnO nanoparticles. Electrochemically ZnO nanoparticles are electroactive by exhibiting charge transfer resistance (R_{ct}) 82006 Ω and bare GCE 3.7707 × 10^5 Ω. Showed good catalytic and conductivity which can be applied for pseudo capacitors.

Keywords: Biological synthesis, Electrodeposition, Nanoparticles, *Sageretia thea*, Glassy carbon electrode.

Received: June 19, 2017; **Accepted:** June 30, 2017; **Published:** July 04, 2017

Introduction

Nanotechnology is emerging as a new field of research dealing with synthesis of nanoparticles (NPs) and nanomaterials for their applications in various fields such as electrochemistry, catalysis, sensors, biomedicines, pharmaceutics, health care, cosmetics, food technology, textile industry, mechanics, optics, electronics, space industry, energy science, optical devices, etc [1-3]. The only reason for using nanotechnology in different fields is its unique capability to enhance the efficiency of the system when it is incorporated with nanotechnology [4]. In nanotechnology, the most usable thing is nanoparticle, also often called "engineered nanomaterial" [2,5]. In common sense nanoparticles are the collections of atom bonded together with smallest sizes as stated above. Another highly attracted property of nanoparticle is its large surface area which makes it more efficient to interact with solvent molecules when it is added for making suspension [6]. Along with this the most significant properties of nanomaterials also include optical transparency, colour change, chemical catalysis, electrical conductivity, thermal properties like heat transfer, cooling, and insulation and property of mechanical strength like ultra-high strength of material [3,7].

Metallic oxide nanoparticles, specifically nano-scale ZnO have gained considerable importance in recent years due to their wide range of applications in various field of science [4,8].

Furthermore, ZnO is an environmentally friendly material, several physical and chemical methods have been developed to obtain ZnO micro- and nanoparticles with different morphology [9]. Numerous strategies such as chemical vapour deposition, electrochemical deposition, hydrothermal solution synthesis, and sol-gel processing have been developed for the synthesis of ZnO nano materials [10-12]. There are several studies that have been reported on ZnO nanoparticles with different applications, there are as follows:

Zinc oxide nanoparticles have been viewed as one of the most promising active materials with high energy density of 650 A h/g for super capacitors, due to its significant advantages of low cost, abundant availability, environment friendly nature and electrochemical activity [9,13,14]. Super capacitors have received increasing attention as energy storage devices in the recent years because of their high-power density, excellent cycle performance, ultrafast charging/discharging rate, low cost and environment friendly [14-16]. Much of research effort has been devoted to achieve high performance super capacitors, and reveals that both of electrode structure and Faradic active materials are very important factors that have significant influence on the capacitance performance [14,17,18].

ZnO nanoparticles have gained momentum in the past decade for providing a broad spectrum in resistance against bacteria. Since bacterial pathogens have been found to develop resistance against antibiotics [6,19,20]. There are only a few reports demonstrating antibacterial activity of ZnO nanoparticles against multiple-antibiotic-resistant (MAR) strains [21]**.** The first evidence of ZnO action against multidrug resistan**ce** S. aureus came, found that the killing ability of zinc oxide against multidrug resistance cells increased in the presence of some common antibiotics such as ciprofloxacillin [6,20,21]. Although the combination therapy is found useful against multidrug resistance bacteria, the exact mechanism of nanoparticle action still remains ambiguous. The mechanism for bactericidal property of ZnO has been described to be the production of Reactive Oxygen Species (ROS) that internalize the bacterial cell envelope and the damage it leads to subsequent cell death. A number of studies have indicated that the primary cause of the antibacterial action might be from the disruption of cell membrane [6,19-21].

Gas sensors constructed with ZnO nanomaterials for instance, have been extensively investigated to detect chemicals, such as ethanol, NO_2 and H_2S [14,22]. Especially, 2D ZnO nanosheets with mesoporous structures exhibit excellent gas sensing properties including high sensitivity, good selectivity and long-term stability [14,22,23]. $Zn_5(OH)_8Cl_2{\cdot}H_2O$, as one type of precursors to topologically produce ZnO nanomaterials, has also attracted attention for their gas sensing applications, such as hydrogen gas sensor with highly improved response of 55 at 300°C [14,23]. It has been reported that ZnO nanoparticles can readily agglomerate, owing to their high surface energy [24]. Therefore, having an applicable strategy to control ZnO-NPs agglomeration, e.g., surfactant coating or capping, is crucial to encounter biofluids [2,5]. In addition, for such biological applications as sensing or drug delivery, the surface of ZnO nanoparticles should be functionalized to preserve water solubility and probe/drugs bioconjugate attachment [6,22,25]. Although, bulky form of ZnO particles have been recognized as generally recognized as safe material by the FDA and many researchers have indicated the low toxicity of their nano-scale form against normal cells, coating of nanoparticles is also an appropriate method for reducing unwanted toxicity and improving biocompatibility of nanoparticles [7,26,27]. To date, a number of capping agents or polymeric compounds have been employed to modify and functionalize ZnO nanoparticles [7,11,28].

These conventional techniques used for synthesis of metal NPs are quite expensive and hazardous to the environment due to involvement of various perilous and hazardous chemicals in their synthesis responsible for various health risks [6,7,29]. During the last decade, researchers showed their interest to biological method involved in synthesis of metal and metal oxide NPs, and the development of this biologically inspired technique is evolving as an important branch in the field of nanotechnology and nanoscience [1,2,30]. In the biological synthesis method, the use of plant extracts, fungi, microbes, and raw materials of fruits and vegetables are used for synthesis of metal and metal oxide NPs [26,31,32]. The various types of NPs have been synthesized by using this green and eco-friendly way using plants extract and microbes [22]. The morphological structure of NPs plays an important role in controlling chemical, physical, and optical properties [33,34].

The plant extracts used were from *Sageretia thea* a member of the family Rhamnacea, a plant common in certain regions of Paskistan. Various phyto-chemical studies carried out on different parts of these tree species show that the extracts obtained from the *Sageretia thea* contained flavonoids, polyphenols, steroids, alkaloids and triterpenoids [1,11].

This study attempts to take advantage of interaction between *Sageretia thea* plant extracts and zinc metal precursor to prepare nano ZnO, reported for the 1st time. Generally, the extracts contain myricetrin, syringic acid, daucosterol, beta-sitosterol, quercetin and glucopyranoside which forms chelation with zinc metals by adsorption to finally form nano ZnO. Apart from the zinc containing precursor, there was no use of inorganic neither organic solvents nor surfactants in this method of synthesis making the process environmentally friendlier. The main purpose is to achieve a deeper insight into a systematic investigation on thermal stability, structural, morphological and electrochemical activity of ZnO nanoparticles. Mechanisms of formation of ZnO nanoparticles via zinc precursor and phytochemical bioactive compounds of the natural extract is proposed.

Methods

Synthesis of ZnO nanoparticles using green extracts

Zinc nitrate hexahydrate ($Zn(NO_3)_2$ $6H_2O$) was purchased from Sigma Aldrich, and *Sageretia thea* leaves was from Pakistan (middle east Africa) [1]. In a typical setup 6.32 g of *Sageretia thea* leaves were heated in 200 ml of deionized water at a temperature

range between 80°C and 90°C for 2 to 3 hours. The green extract with a pH of 3.92 was filtered after cooling to room temperature and added 1.623 g of ($Zn(NO_3)_2$ $6H_2O$) Zinc nitrate hexahydrate salt. The extract with the metal precursor was heated to 90°C for 1 hour under constant stirring with a magnetic stirrer. The salt was observed to have completely dissolved in the aqueous extract with a formation of a brown precipitate. The precipitate was separated from the aqueous extract by decanting then by centrifuging at 3500 rpm 3 times to 4 times over washing the precipitate with deionised water. Subsequently calcination was carried out at 300°C and 500°C for 2 hours in open air, obtained highly crystalline nanocrystals white in colour which was later confirmed by structural analysis. Phytochemicals of *Sageretia thea* are known to be phenolic acid, flavonoids, natural sterolin and vitamin based compounds [1,35].

Characterization techniques

Various techniques were used to characterize and investigate thermal stability, structural, morphological and electrochemical activity of ZnO nanoparticles. The phase identification of the annealed powders ZnO was performed on an X-Ray Diffraction (XRD) Model Bruker AXS D8 advance with radiation $\lambda Cuk_{\alpha 1}$=1.5406Å. A simultaneous differential scanning calorimetry/thermogravimetric analysis (DSC/TGA) was used to characterize the decomposition and thermal stability of nanoparticles measured from 50°C to 500°C at the heating rate of 10°C/min. A Fourier transform infrared (FT-IR) absorption spectrometer (Shimadzu 8400 s spectrophotometer, 400 cm^{-1} to 4000 cm^{-1}) as well as Raman measurements (LabRam HR by Jobin-Yvon Horiba scientific Explora, France) with a 1200 line mm^{-1} grating coupled to a microscope (Model BX41, Olympus). High Resolution Transmission Electron Microscopy (HRTEM) analysis was carried out on a Philips Technai TEM instrument operated at an accelerating voltage of 120 kV. The Energy Dispersive Xray Spectroscopy (EDS) was performed on an EDS Oxford instrument for elemental analysis.

Electrochemistry

All electrochemical measurements were carried out using a Potentiostat/Galvanostat Autolab 30 equipped with a Frequency Response Analyzer (FRA 4.9). This was then interfaced with a personal computer and controlled by GPES 4.9 and FRA 4.9 software (Eco Chemie, B.V., Utrecht, The Netherlands). Used a conventional three-electrode system consisting of a 1.0 mm Glassy Carbon Electrode (GCE) as the working electrode, platinum wire as the auxiliary electrode and Ag/AgCl (with 3 M NaCl salt bridge) as the reference electrode. The cyclic voltammetry (CV) was recorded under argon atmosphere. The GCE/ZnO electrode was prepared by dissolving ZnO nanoparticles in ethanol, the solution was ultra-sonicated using a warm bath for 10 mins. Alumina micro polish (1.0 mm, 0.3 mm and 0.05 mm alumina slurries) and polishing pads (Buehler, IL, USA) were used for polishing the working electrode (GCE) surface before and after measurements. The 4 µL of the solution was drop coated on the surface area of GCE and dried in the oven at 20°C for 30 mins. All the electrochemical experiments were deoxygenated by bubbling with highly purified argon gas for 20 mins and blanketed with argon throughout the experiment.

Electrochemical measurements were performed in 10 mL of 0.1 M H_2SO_4 electrolyte over a potential range of -900 mV to +100 mV the solution was used as the test solution for ZnO nanoparticles. Electrochemical impedance spectroscopy (EIS) of the nanoparticles modified electrodes were measured in 0.1 M H_2SO_4 at a perturbation amplitude of 10 mV within a frequency range of 100 kHz to 100 mHz.

Results and Discussion

X-Ray diffraction (XRD)

Figure 1 The crystal structure of prepared ZnO at room temperature and annealed at 300°C and 500°C were confirmed using X-ray diffraction. The spectra of the non-annealed nano powder displayed an amorphous signature. The annealed nano powder showed peaks that can be indexed to the hexagonal wurtzite structure ZnO, which coincide with the standard JCPDS card (No.36-1451) [4,7,36]. The Bragg peaks are ascribed to crystallographic reflection from the (100), (002), (101), (102), (110), (103), (200), (112), (201) and (202) plane [37]. The strong sharp diffraction peak indicate that ZnO nanoparticles annealed at 500°C are well crystallized [6,31]. The crystallite size of ZnO nanoparticles were calculated from peak broadening of diffraction peak using Scherrer formula [9,17,38,39].

$$D = \frac{k\lambda}{\beta \cos\theta_B} \quad (1)$$

In this equation 1, λ represents the wavelength of X-ray radiation, β is the full width and half maximum of the diffraction peak and Θ_B the Bragg's angle. The average crystallite size of ZnO nanoparticles annealed at 500°C was 31.03 nm and for ZnO annealed at 300°C was 25.15 nm. The crystal structure of ZnO annealed at 300°C and 500°C is Wurtzite in which the oxygen atoms are arranged in a hexagonal close packed type with Zn atoms occupying half of the tetrahedral sites. The Zn and O atoms are in tetrahedral coordination to each other. The lattice

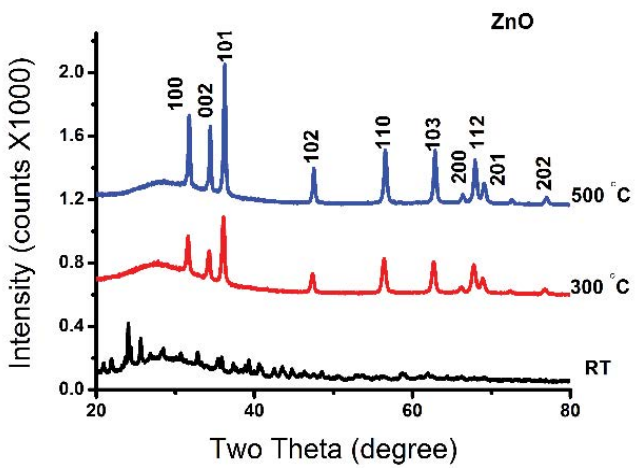

Figure 1 XRD patterns of ZnO nanoparticles annealed at 300°C and 500°C.

parameter of ZnO hexagonal structure and the plane spacing d_{hkl} is related to the lattice constant a, c and the miller indices by [22,35,39].

$$\frac{1}{d_{hkl}^2} = \frac{4}{3}\left(\frac{h^2+hk+k^2}{a^2}\right) + \frac{l^2}{c^2} \quad (2)$$

The lattice parameter was calculated using the above equation with the Bragg's law ($2d_{hkl}\sin\Theta=n\lambda$), we calculated the values of "a" and "c". The lattice constant calculated from (101) peak. The value of "a" for ZnO NP/500° C and ZnO NP/300°C was 3.247 and 3.253 Å and "c" was 5.206 and 5.202 Å respectively. The XRD suggest that on set crystallization does not begin until ≈ 300°C before which ZnO nano-powder produced is amorphous.

Thermogravimetric Analysis TGA/Differential Scanning Calorimetry (DSC)

Figure 2 reports a typical DSC/TGA curves of the biosynthesized ZnO based product heated at 10°C/min. thermogravimetric analysis is a process in which a substance is decomposed in the presence of heat which causes bonds within the molecules to be broken [28,36]. The TGA profile exhibits continuous weight loss with 3 quasi sharp changes occurring at 79°C, 228°C and 300°C followed by constant plateau. The first decomposition step with a percentage weight loss of (10.1%) may be due to desorption of physically adsorbed water. The second and third decomposition with a weight loss percentage of (21.3% and 30.7%) is due to chemically absorbed water, alcohol, organic matter and the hydroxide group [5,35,36]. Hence annealing at above 350°C guarantee the formation of ZnO nanoparticles. The DSC curve of the biosynthesized ZnO nanoparticle revealed 3 endothermic peaks at 79°C, 228°C and 300°C. The peak at 79°C might be due to loss of volatile surface molecules adsorbed. The peak at 228°C is due to the conversion of Zinc complex to Zinc hydroxide. Lastly the peak at 300°C is due to the formation of Zinc Oxide nanoparticles and decomposition of organic matter [35,36]

High Resolution Transmission Electron Microscope (HRTEM)

Figure 3 reports a typical High-Resolution Transmission Electron Microscope (HRTEM), Energy Dispersive X-Ray (EDX) as well as Selected Area Electron Diffraction (SAED) of ZnO nanoparticles annealed at 500°C in air. **Figure 3a** shows that the particles were highly agglomerated quasi-spherical in shape [37]. The average diameter of the nanoparticles was found to be of the order of ($f_{particles}$) ≈ 28.09 ± 5 nm. To conclude on the degree of crystallinity of the nanoparticles, several HRTEM and SAED analysis were carried out (**Figures 3b and 3c**). The bulk of the nanoparticles appear to be polycrystalline [11,23]. The reticular distance of the observed lattice fringe is 0.29 nm which is in good agreement with ZnO [100] (d_{100}=0.287 nm) interreticular plane distance [40]. In **Figure 3d** reports the EDX analysis of ZnO nanoparticles, distinct peaks of O, Zn and Cu are present. Zn and O are related to ZnO nanoparticle while Cu is due to the copper grid on which the nanoparticles were drop coated to minimize electrons from charging [10,39].

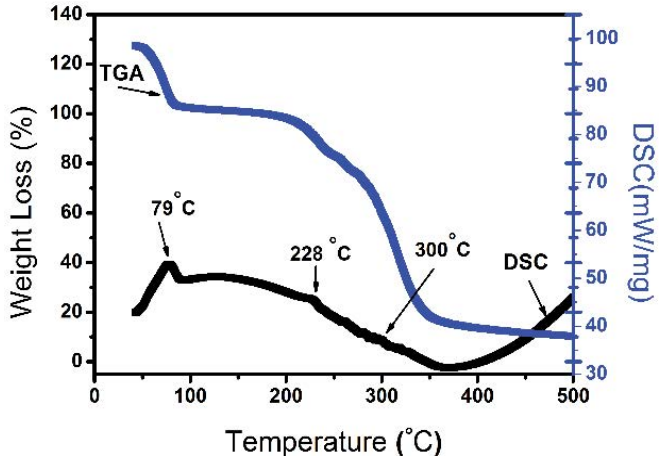

Figure 2 Simultaneous TGA/DSC of ZnO nanoparticles before annealing.

Fourier Transform Infrared (FTIR) and proposed mechanism of reaction

FTIR was used to confirm the nature of ZnO nanoparticles, composition and functional groups at the surface in order to identify the potential ZnO mechanism of formation. A study was carried out on the *Sageretia thea* natural extracts and the biosynthesised Zn based product and an annealed ZnO nanoparticles at 300°C and 500°C. **Figure 4** showed absorption bands for ZnO RT 2685 cm^{-1}-3553 cm^{-1} can be assigned to C=C, O-H, COOH and OCH_3, absorption band at 1239 cm^{-1}-1903 cm^{-1} can be assigned to C=O, CH_3 and C=C aromatic of various bioactive compound of *Sageretia thea* natural extract as shown in **Figure 5**. Before and after the process of annealing it can be seen from the spectra that there is an intrinsic absorption band below 1000 cm^{-1} in the finger print region arising from inter-atomic vibrations [35,41]. The absorption peak at 457 cm^{-1} is associated to the stretching mode of ZnO nanoparticles at RT, annealed at 300°C and 500°C. after annealing the FTIR spectrum indicated no significant absorption peaks at higher wavelength, indicating the nature of nanoparticles formed [35,41,42].

In **Figure 5** major bioactive compounds present in *Sageretia thea* extracts are shown in order to bring understanding how metal precursor salt ($Zn(NO_3)_2$. $6H_2O$) can transform in to ZnO nanoparticles. The action of different biological compounds as both chelating and capping agents, the proposed mechanism of reaction shows how [1,2,30]. Glucopyranoside has been chosen as a representative compound to propose the mechanism. The aromatic hydroxyl group adhere to zinc ions which lead to a stable complex of zinc and glucopyranoside. After the process of annealing the complex decomposes to give rise to ZnO nanoparticles. Polyphenolic compound such as myricetrin and syringic acid are responsible for bioreduction [6,8,32]. The presents of a carboxylic group it stabilizes the ZnO nanoparticle and prevents growth [1,35,43].

Raman spectroscopy

Raman scattering is a useful technique to investigate the nanomaterials [11]. **Figure 6** shows the RT Raman spectra of

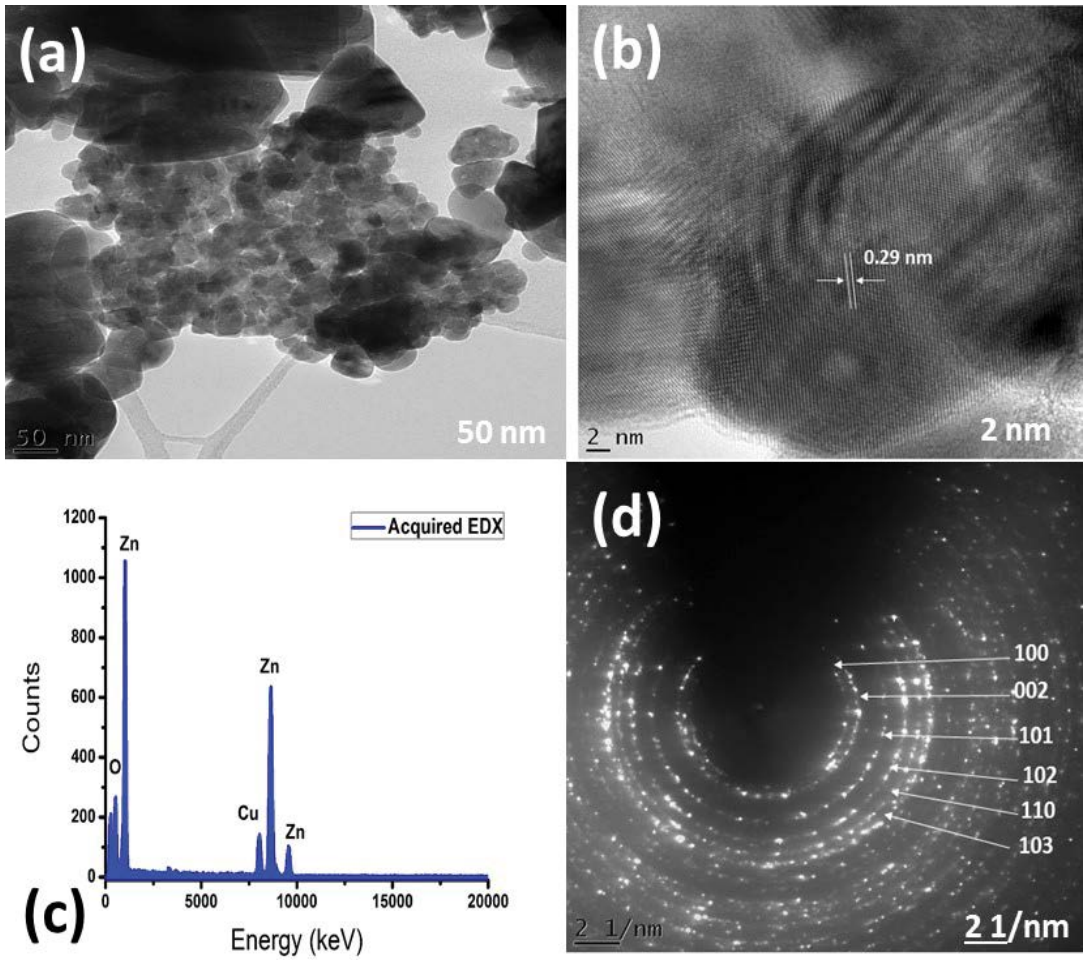

Figure 3 (**a**) and (**b**) HRTEM image of ZnO annealed at 500°C, (**c**) EDX spectra of ZnO annealed at (**d**) 500°C and Selected electron diffraction patterns of ZnO nanoparticles annealed at 500°C.

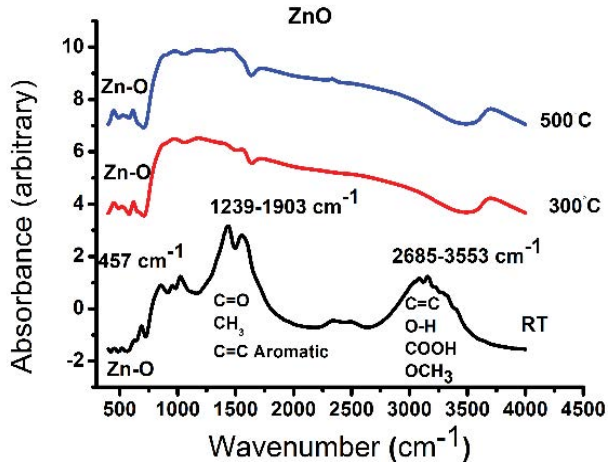

Figure 4 FTIR spectra of *Sageretia thea* extracts and ZnO nanoparticles annealed at 300°C and 500°C.

ZnO nanoparticles at RT, annealed at 300°C and 500°C. Samples shows a higher peak at 483 cm^{-1} (ZnO RT), 492 cm^{-1} (ZnO 300°C) and 483 cm^{-1} (ZnO 500°C) which can be assigned to the E_2 (high) vibration mode of the ZnO non-polar optical photons [44]. The high intensity of the E_2 mode and the weak $2E_2$ mode (370 cm^{-1}; ZnO 300°C and 329 cm^{-1}, 375 cm^{-1}; ZnO 500°C) indicate the high crystallinity of ZnO [45]. The peak at 531 cm^{-1}, 571 cm^{-1} (ZnO 300°C) and 579 cm^{-1} (ZnO 500°C) can be assigned to $A_{1(LO)}$ and $E_{1(LO)}$ vibration mode. The sample absorption maybe the reason for the decrease of the Raman peaks [4,46,47]. The broadened weak peak at 579 cm^{-1} (ZnO 500°C) appeared in the spectra is usually related with the defects of the O-vacancy and Zn interstitial [4,11].

Electrochemical study

Figure 7 shows the electrochemical performance of ZnO nanoparticles annealed at 500°C drop coated on GCE were investigated by cyclic voltammetry (CV) in 0.1 M H_2SO_4 electrolyte.

The ZnO nanoparticles displayed good reactivity in the potential window -900 mV to +100 mV from the scan rate was 20 $mV.s^{-1}$, 40 $mV.s^{-1}$, 60 $mV.s^{-1}$, 80 $mV.s^{-1}$ till 100 $mV.s^{-1}$, respectively. The increase in the current density with the increase in the potential scan rate is attributed to the excitation signal caused during the charging of the interface capacitance by the charge transfer process. Thus, showing the CV for bare GCE and ZnO nanoparticles at different scan rates [35,48]. The shape of the curves is nearly

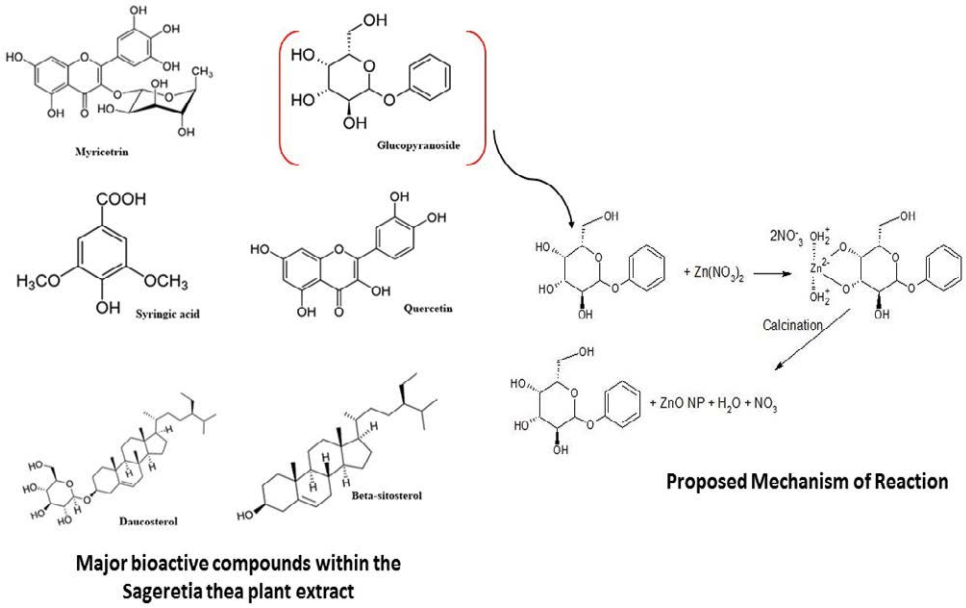

Figure 5 Schematic diagram of major bioactive compounds within the *Sageretia thea* plant extract and proposed mechanism of reaction with a representative compound.

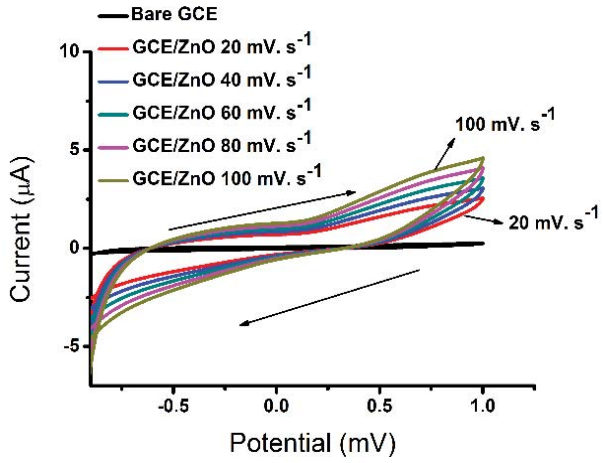

Figure 6 Cyclic voltammogram in test solution 0.1 M H_2SO_4 of ZnO nanoparticles modified on glassy carbon electrode (GCE/ZnO) at different scan rates; 20 $mV.s^{-1}$, 40 $mV.s^{-1}$, 60 $mV.s^{-1}$, 80 $mV.s^{-1}$, and 100 $mV.s^{-1}$ respectively.

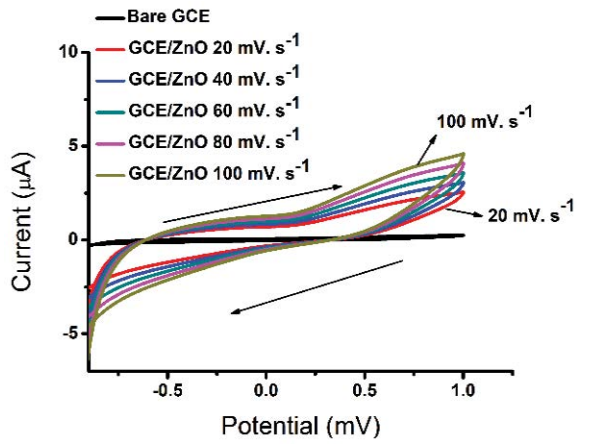

Figure 7 Cyclic voltammogram in test solution 0.1 M H_2SO_4 of ZnO nanoparticles modified on glassy carbon electrode (GCE/ZnO) at different scan rates; 20 $mV.s^{-1}$, 40 $mV.s^{-1}$, 60 $mV.s^{-1}$, 80 $mV.s^{-1}$, and 100 $mV.s^{-1}$ respectively.

rectangular show clear increase in current with scan rate which suggests the contribution from faradaic reaction [15,31]. It is further interesting to note that CV curves remain unchanged as scan rate increase thus indicating the excellent electrochemical reversibility and exceptional high rate performance [49]. The electrode exhibits relatively high current density, corresponding to high capacitance which might be attributed to its morphology and good conductivity [33,35,50].

Figure 8a the charge transfer resistance (R_{ct}) of ZnO NP was the lowest (R_{ct}=82006 Ω) compared to that of bare GCE working electrode (3.7707 x 10^5 Ω), indicating that the ZnO nanoparticles have good conductivity as compared to bare GCE and played an important role in accelerating the transfer of electrons [38,47]. This can be attributed to the increased catalytic and improved conductivity properties portrayed by nanoparticles. Electrochemical Impedance Spectroscopy (EIS) is a very powerful tool used to investigate the electrochemical characteristics of the electrode/electrolyte interface using a Nyquist plot, which is a representation of the real and imaginary parts of the impedance in a sample [51,52]. The impedance parameters were obtained by fitting using an equivalent circuit and the fitting errors were less than 2%.

In **Figure 8b** shows plots of phase angle changes with frequency for ZnO nanoparticles. Bode plots showed remarkable electronics

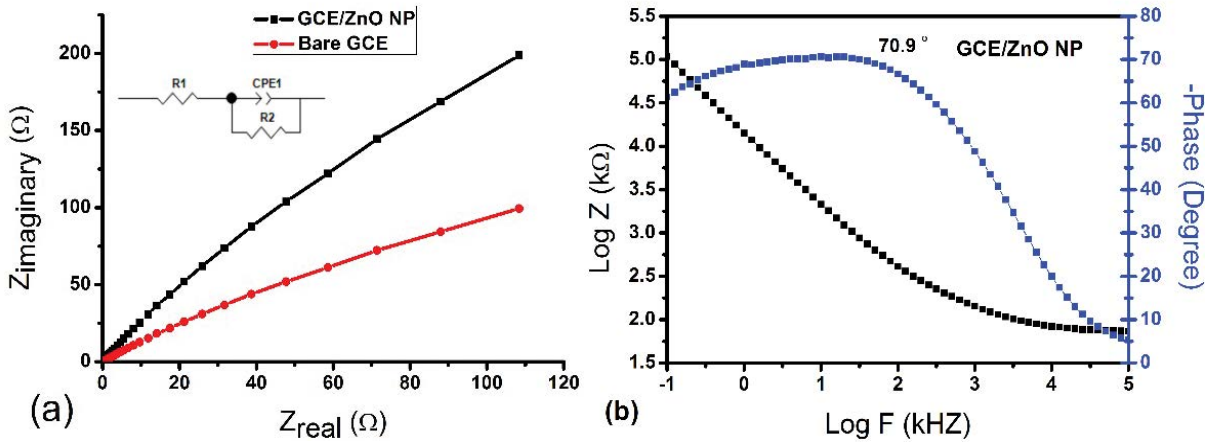

Figure 8 Electrochemical impedance spectroscopic (**a**) Nyquist plot and (**b**) Bode plot of ZnO nanoparticles modified on glassy carbon electrode (GCE/ZnO) tested in 0.1 M H_2SO_4.

of ZnO nanoparticles interfaces. The frequency of maximum phase angle increased with the phase angle decreasing to semiconductor value of (70.9˚) for ZnO nanoparticles [53]. The Bode plot gives direct information on the frequency and phase angle. The frequency at maximum phase is a useful parameter in determining the double layer capacitance. In most applications however, analysis of both Bode and Nyquist plots is highly advised in order to conclusively study electrochemical processes at interfaces [52,54,55].

Conclusion

In summary, ZnO nanoparticles were successfully biosynthesised using natural green extracts of *Sageretia thea* with an average particle size of 28.09 ± 5 nm. The XRD patterns of the sample show ZnO annealed at 300°C and 500°C exhibit wurtzite structure with no secondary phases. The ZnO after synthesis was amorphous after heat treatment significant crystallization was observed at 300°C and 500°C. The TGA exhibited weight loss were 3 quasi sharp changes and DSC exhibited 3 endothermic peaks at 79°C, 228°C and 300°C were heat causes bonds within the molecules to be broken. HRTEM showed ZnO to be nanoparticulate and polycrystalline with EDX showing composition of the material. FTIR spectra was used to propose a possible mechanism were biological compounds act as both chelating and capping agents. The Zn^{2+} ions are considered to react with phytochemicals of *Sageretia thea* which are phenolic acid, flavonoids, natural sterolin and vitamin based compounds to form nanoparticles. Raman spectrum showed a red shift and broad features in all peaks which can be ascribed to a quantum confinement effect observed in nanosized ZnO. The voltammetric studies showed that the GCE/ZnO electrode exhibits relatively high current density, corresponding to high capacitance. The EIS showed ZnO nanoparticles has good catalytic and conductivity while the bode plot proved that the material is a semiconductor. Electrochemical activity of the material showed that it can be used as an electrocatalyst or applied for pseudo capacitors. This method demonstrated that natural extracts can be used as a cost effective, eco-friendly alternative in preparation of metal oxides nanoparticles, in this instance ZnO.

Acknowledgements

This research work was funded by South African Nuclear Human Asset and Research Programme (SANHARP), National Research Foundation (NRF), Department of Science and Technology (DST), iThemba LABS, University of The Western Cape and UNESCO-UNISA-Africa Chair in Nanoscience and Nanotechnology.

References

1 Ahmed SA, Chaudhry SA, Ikram S (2017) A review on biogenic synthesis of ZnO nanoparticles using plant extracts and microbes: A prospect towards green chemistry. J Photochem Photobiol B Biol 166: 272-284.

2 Aladpoosh R, Montazer M (2015) The role of cellulosic chains of cotton in biosynthesis of ZnO nanorods producing multifunctional properties: Mechanism, characterizations and features. Carbohyd Polym 126: 122-129.

3 Bera A, Belhaj H (2016) Application of nanotechnology by means of nanoparticles and nanodispersions in oil recovery- A comprehensive review. J Natural Gas Sci Eng 34: 1284-1309.

4 Alim KA, Fonoberov VA, Shamsa M, Balandin AA (2005) Micro-Raman investigation of optical phonons in ZnO nanocrystals. J Appl Phys 97: 124313-124317.

5 Dejene FB, Ali AG, Swart HC, Botha RJ, Roro K, et al. (2011) Optical properties of ZnO nanoparticles synthesized by varying the sodium hydroxide to zinc acetate molar ratio using sol gel process. Cent Eur J Phys 9: 1321-1326.

6 Elumalai K, Velmurugan S, Ravi S, Kathiravan V, Ashokkumar S (2015) Green synthesis of zinc oxide nanoparticles using Moringa oleifera leaf extract and evaluation of its antimicrobial activity. Spectrochim. Acta A Mol Biomol Spectrosc. 143: 158-164.

7 Dong Y, Jiao Y, Jiang B, Tian C (2017) Commercial ZnO and its hybrid with Ag nanoparticles: Photocatalytic performance and relationship with structure. Chem Phys Lett 679: 137-145.

8 Iravani S (2011) Green synthesis of metal nanoparticles using plants. Green Chem 13: 2638-2650.

9 Jiang J, Li Y, Liu J, Huang X, Yuan C (2012) Recent advances in metal oxide-based electrode architecture design for electrochemical energy storage. Adv Mater 24: 5166-5180.

10 Rajabi HR, Naghiha R, Kheirizadeh M, Sadatfaraji H, Mirzaei A, et al. (2017) Microwave assisted extraction as an efficient approach for biosynthesis of zinc oxide nanoparticles: Synthesis, characterization, and biological properties. Mater Sci and Eng 78: 1109-1118.

11 Sone BT, Manikandan E, Gurib FA, Maaza M (2015) Sm2O3 nanoparticles green synthesis via Callistemon viminalis' extract. J Alloy Compd 650: 357-362.

12 Vijayakumar S, Vaseeharan B, Malaikozhundan B, Shobiya M (2016) Laurus nobilis leaf extract mediated green synthesis of ZnO nanoparticles: Characterization and biomedical applications. Biomed Pharmacother 84: 1213-1222.

13 Wu DY, Li JF, Ben B, Tian ZQ (2008) Electrochemical surface enhanced Raman spectroscopy of nanostructures. Chem Soc Rev 37:1025-1041.

14 Zhang Y, Liu C, Gong F, Jiu B, Li F (2017) Large scale synthesis of hexagonal simonkolleit nanosheets for ZnO gas sensors with enhanced performances. Matt Lett 186: 7-11.

15 Tajik S, Dubal DP, Gomez RP, Yadegari A, Rashidi A, et al. (2017) Nanostructured mixed transition metal oxides for high performance asymmetric supercapacitors: Facile synthetic strategy. Int J Hydrogen Energy 42: 12384-12395.

16 Zhu D, Fu YM, Zang WL, Zhao YY, Xing LL, et al. (2014) Piezo/active humidity sensing of CeO2/ZnO and SnO2/ZnO nanoarray nano-generators with high response and large detecting range. Sens Actuators B 205: 12-19.

17 He G, Fan H, Ma L, Wang K, Liu C, et al. (2016) Dumbbell-like ZnO nanoparticles-CeO2 nanorods composite by one-pot hydrothermal route and their electrochemical charge storage. Appl Surf Sci 366: 129-138.

18 Pang H, Ma YH, Li GC, Chen J, Zhang JS, et al. (2012) Facile synthesis of porous ZnO-NiO composite micro-polyhedrons and their application for high power super capacitor electrode materials. Dalton Trans 41: 13284-13291

19 Chung M, Rahuman AA, Marimuthu S, Kirthi AVA, Anbarasan K, et al. (2015) An investigation of the cytotoxicity and caspase-mediated apoptotic effect of green synthesized zinc oxide nanoparticles using Eclipta prostrata on human liver carcinoma cells. Nanomater 5: 1317-1330.

20 Karthik R, Thambidurai S (2017) Synthesis of cobalt doped ZnO/reduced graphene oxide nanorods as active material for heavy metal ions sensor and antibacterial activity. J Alloy Compd 715: 254-265.

21 Sharma D, Sabela MI, Kanchi S, Mdluli PS, Singh G, et al. (2016) Biosynthesis of ZnO nanoparticles using *Jacaranda mimosifolia* flowers extract: Synergistic antibacterial activity and molecular simulated facet specific adsorption studies. J Photochem Photobiol 162: 199-207.

22 Lamberti A, Sacco A, Laurenti M, Fontana M, Pirri CF, et al. (2014) Sponge-like ZnO nanostructures by low temperature water vapor-oxidation method as dye-sensitized solar cell photoanodes. J Alloy Compd 615: S487-S490.

23 Fang F, Futter J, Markwitz A, Kennedy J (2009) UV and humidity sensing properties of ZnO nanorods prepared by the arc discharge method. Nanotechnol 20: 245-502.

24 Guillemin JP, Schaer E, Marchal P, Lemaître C, Nonnet H, et al. (2012) A mass conservative approach to model the ultrasonic de-agglomeration of ZnO nanoparticle suspension in water. Powder Technol 219: 59-64.

25 Lang J, Zhang Q, Han Q, Fang Y, Wang J, et al. (2017) The study of structural and optical properties of (Eu, La, Sm) codoped ZnO nanoparticles via a chemical route. Mater Chem Phys 194: 29-36

26 Jacob JM, Sharma S, Balakrishnan RM (2017) Exploring the fungal protein cadre in the biosynthesis of PbSe quantum dots. J Hazard Mater 324: 54-61

27 Sundrarajan M, Ambika S, Bharathi K (2015) Plant-extract mediated synthesis of ZnO nanoparticles using *Pongamia pinnata* and their activity against pathogenic bacteria. Adv Powder Technol 26: 1294-1299.

28 Darezereshki E, Alizadeh M, Bakhtiari F, Schaffie M, Ranjbar M (2011) A novel thermal decomposition method for the synthesis of ZnO nanoparticles from low concentration ZnSO4 solutions. Appl Clay Sci 54: 107-111.

29 Wang G, Zhang L, Zhang J (2012) A review of electrode materials for electrochemical supercapacitors. Chem Soc Rev 41: 797-828.

30 Çolak H, Karaköse E (2017) Green synthesis and characterization of nanostructured ZnO thin films using *Citrus aurantifolia* (lemon) peel extract by spin-coating method. J Alloy Compd 690: 658-662.

31 Fang L, Liu B, Liu L, Li Y, Huang K, et al. (2016) Direct electrochemistry of glucose oxidase immobilized on Au nanoparticles-functionalized 3D hierarchically ZnO nanostructures and its application to bioelectrochemical glucose sensor. Sens Actuators B: Chem 222: 1096-1102.

32 Karnan T, Selvakumar SAS (2016) Biosynthesis of ZnO nanoparticles using rambutan (*Nephelium lappaceum* L.) peel extract and their photocatalytic activity on methyl orange dye. J Mol Struct 1125: 358-365.

33 Liu J, Guo C, Li CM, Li Y, Chi Q, et al. (2009) Carbon-decorated ZnO nanowire array: A novel platform for direct electrochemistry of enzymes and biosensing applications. Electrochem Commun 11: 202-205.

34 Thirumavalavan M, Huang KL, Lee JF (2013) Preparation and morphology studies of nano Zinc Oxide obtained using native and modified chitosans. Mater 6: 4198-4212.

35 Matinise N, Fuku XG, Kaviyarasu K, Mayedwa N, Maaza M (2017) ZnO nanoparticles via *Moringa oleifera* green synthesis: Physical properties and mechanism of formation. Appl Surf Sci 406: 339-347.

36 El-Kader FHA, Hakeem NA, Elashmawi IS, Ismail AM (2013) Structural, optical and thermal characterization of ZnO nanoparticles doped in PEO/PVA blend films. Nanosci Nanotechnol 7: 179-188.

37 Lingaraju K, Naika HR, Manjunath K, Basavaraj RB, Nagabhushana H, et al. (2015) Biogenic synthesis of zinc oxide nanoparticles using *Ruta graveolens* (L.) and their antibacterial and antioxidant activities. Appl Nanosci 1: 1-8.

38 Huang X, Qi XY, Boey F, Zhang H (2012) Graphene-based composites. Chem Soc Rev 41: 666-686

39 Javed R, Usman M, Tabassum S, Zia M (2016) Effect of capping agents: Structural, optical and biological properties of ZnO nanoparticles. Appl Surf Sci 386: 319-326.

40 Manjunath K, Ravishankar TN, Kumar D, Priyanka KP, Varghese T, et al. (2014) Facile combustion synthesis of ZnO nanoparticles using *Cajanus cajan* (L.) and its multidisciplinary applications. Mater Res Bull 57: 325-334.

41 Habibi MH, Rahmati MH (2014) Fabrication and characterization of ZnO@CdS core–shell nanostructure using acetate precursors: XRD, FESEM, DRS, FTIR studies and effects of cadmium ion concentration on band gap. Spectrochim Acta Part A: Mol Biomol Spectrosc 10: 13-18

42 Gharagozlou M, Naghibi S (2016) Sensitization of ZnO nanoparticle by vitamin B12: Investigation of microstructure, FTIR and optical properties. Mater Res Bull 84: 71-78.

43 Krishnaswamy K, Orsat V (2015) Insight into the nanodielectric properties of gold nanoparticles synthesized from maple leaf and pine needle extracts. Ind Crops Prod 66: 131-136.

44 Yi Z, Xu X, Kang X, Zhao Y, Zhang S, et al. (2017) Fabrication of well-aligned ZnO @ Ag nanorod arrays with effective charge transfer for surface-enhanced Raman scattering. Surf Coatings Technol 324: 257-263

45 Zhang QY, Ashfaq JM, Hu BC, Wang JY, Zhou N (2016) Enhanced resonant Raman scattering and optical emission of ZnO/ZnMgO multiple quantum wells. J Alloy Compd 680: 232-236.

46 Prakash O, Gautam P, Singh RK (2015) Probing the orientations of coordination complex molecules onto the surface of ZnO nanoparticles by means of surface enhanced Raman scattering, UV–vis and DFT methods. Appl Surf Sci 349: 657-664.

47 Zhang Y, Zhang Y, Wang H, Yan B, Shen G, et al. (2009) An enzyme immobilization platform for biosensor designs of direct electrochemistry using flower-like ZnO crystals and nano-sized gold particles. J Electroanal Chem 627: 9-14.

48 Frasca S, Milan AM, Guiet A, Goebel C, Pérez-Caballero F, et al. (2013) Bioelectrocatalysis at mesoporous antimony doped tin oxide electrodes-Electrochemical characterization and direct enzyme communication. Electrochim Acta 110: 172-180.

49 Zhang F, Wang X, Ai S, Sun Z, Wan Q, et al. (2004) Immobilization of uricase on ZnO nanorods for a reagentless uric acid biosensor. Anal Chim Acta 519: 155-160.

50 Londhe PU, Chaure NB (2017) Effect of pH on the properties of electrochemically prepared ZnO thin films. Mater Sci Semicond Process 60: 5-15.

51 Janáky C, Rajeshwar K (2015) The role of (photo)electrochemistry in the rational design of hybrid conducting polymer/semiconductor assemblies: From fundamental concepts to practical applications. Prog Polym Sci 43: 96-135.

52 Winiarski J, Tylus W, Szczygieł B (2016) EIS and XPS investigations on the corrosion mechanism of ternary Zn-Co-Mo alloy coatings in NaCl solution. Appl Surf Sci 364: 455-466.

53 Shan C, Yang H, Song J, Han D, Ivaska A, et al. (2009) Direct electrochemistry of glucose oxidase and biosensing for glucose based on graphene. Anal Chem 81: 2378-2382.

54 Pahlavan A, Gupta VK, Sanati AL, Karimi F, Yoosefian M, et al. (2014) ZnO/CNTs nanocomposite/ionic liquid carbon paste electrode for determination of noradrenaline in human samples. Electrochim Acta 123: 456-462.

55 Phelane L, Muya FN, Richards HL, Baker PGL, Iwuoha EI (2014) Polysulfone nanocomposite membranes with improved hydrophilicity. Electrochim Acta 128: 326-335.